The LINC complex is required for endothelial cell adhesion and adaptation to shear stress and cyclic stretch

Kevin B. Denis, Jolene I. Cabe, Brooke E. Danielsson, Katie V. Tieu, Carl R. Mayer, and Daniel E. Conway*

Department of Biomedical Engineering, Virginia Commonwealth University, Richmond, VA 20284

ABSTRACT The Linker of Nucleoskeleton and Cytoskeleton (LINC) complex is a structure consisting of nesprin, SUN, and lamin proteins. A principal function of the LINC complex is anchoring the nucleus to the actin, microtubule, and intermediate filament cytoskeletons. The LINC complex is present in nearly all cell types, including endothelial cells. Endothelial cells line the innermost surfaces of blood vessels and are critical for blood vessel barrier function. In addition, endothelial cells have specialized functions, including adaptation to the mechanical forces of blood flow. Previous studies have shown that depletion of individual nesprin isoforms results in impaired endothelial cell function. To further investigate the role of the LINC complex in endothelial cells we utilized dominant negative KASH (DN-KASH), a dominant negative protein that displaces endogenous nesprins from the nuclear envelope and disrupts nuclear-cytoskeletal connections. Endothelial cells expressing DN-KASH had altered cell-cell adhesion and barrier function, as well as altered cell-matrix adhesion and focal adhesion dynamics. In addition, cells expressing DN-KASH failed to properly adapt to shear stress or cyclic stretch. DN-KASH-expressing cells exhibited impaired collective cell migration in wound healing and angiogenesis assays. Our results demonstrate the importance of an intact LINC complex in endothelial cell function and homeostasis.

Monitoring Editor Dennis Discher University of Pennsylvania

Received: Nov 9, 2020 Revised: Jun 22, 2021 Accepted: Jun 25, 2021

INTRODUCTION

In nearly all cells the nucleus is connected to the cytoskeleton by the Linker of Nucleoskeleton and Cytoskeleton (LINC) complex. The LINC complex is made up of two protein families: 1) nesprins (KASH domain proteins), transmembrane proteins on the outer nuclear envelope, and 2) SUN transmembrane proteins on the inner nuclear envelope (Alam et al., 2014). This structure has been shown to regulate nuclear movement and positioning (Luxton et al., 2010; Petrie et al., 2012), DNA repair (Lei et al., 2012; Lottersberger et al., 2015),

and transmission of mechanical forces from the cell surface to the nucleus (Chambliss et al., 2013; Tajik et al., 2016; Mayer et al., 2019). More recently our group showed that the LINC complex is important in the mechanical stability of epithelial glandular acini (Zhang et al., 2019), suggesting that the LINC complex also has an important role in the mechanical stability of multicellular tissues.

Endothelial cells line the surfaces of blood vessels, providing both a barrier and an anti-thrombotic surface. Endothelial cells have been shown to be an especially mechanoresponsive cell type, in particular being highly responsive to two major physiological forces: 1) fluid shear stress, or the frictional drag of blood flow on the vessel wall, and 2) cyclic circumferential stretch due to both the pulsatility of blood flow and blood vessel vasodilation. Although focal adhesions (Hahn et al., 2011; Al-Yafeai et al., 2018) and cell-cell junctions (Tzima et al., 2005; Conway et al., 2013; Abiko et al., 2015) in endothelial cells have been shown to have important roles in sensing and adapting to the mechanical forces of blood flow, there is less known about the nucleus as a potential mechanosensory element in these cells. Interestingly, the endothelial nucleus has also been shown to be affected by shear stress (Hazel and Pedley, 2000; Stamatas and McIntire, 2001; Deguchi et al., 2005; Tkachenko et al., 2013),

This article was published online ahead of print in MBoC in Press (http://www.molbiolcell.org/cgi/doi/10.1091/mbc.E20-11-0698) on June 30, 2021.

*Address correspondence to: Daniel E. Conway (dconway@vcu.edu).

Abbreviations used: AV, adenovirus; DN, dominant negative; ECM, extracellular matrix; FAK, focal adhesion kinase; FRET, Förster resonance energy transfer; FSS, fluid shear stress; HUVEC, human umbilical vein endothelial cells; KASH, Klarsicht, ANC-1, Syne homology; LINC, Linker of Nucleoskeleton and Cytoskeleton.

© 2021 Denis et al. This article is distributed by The American Society for Cell Biology under license from the author(s). Two months after publication it is available to the public under an Attribution–Noncommercial–Share Alike 3.0 Unported Creative Commons License (http://creativecommons.org/licenses/by-nc-sa/3.0).

"ASCB®," "The American Society for Cell Biology®," and "Molecular Biology of the Cell®" are registered trademarks of The American Society for Cell Biology.

1654 | K. B. Denis et al.

suggesting that nuclear-cytoskeletal interactions may be important in endothelial mechanobiology.

The mammalian genome encodes six KASH proteins (nesprins 1–4, KASH5, and LRMP) (Alam et al., 2014). Previous work has shown that endothelial cells express nesprin-1, nesprin-2, and nesprin-3 isoforms (Chancellor et al., 2010; Morgan et al., 2011; Anno et al., 2012; King et al., 2014). Nesprin-1 and -2 giant isoforms connect both actin and microtubules to the LINC complex, whereas nesprin-3 connects intermediate filaments to the nucleus. Depletion of nesprin-1 results in an increased number of focal adhesions, increased traction forces, and decreased migration speed, as well as impaired adaptation to cyclic strain (Chancellor et al., 2010). Nesprin-1 depletion also increases both nuclear width and nuclear deformations induced by cyclic stretch (Anno et al., 2012). In a subsequent study of both nesprin-1 and nesprin-2 isoforms it was found that depletion of either isoform reduced endothelial migration, impaired angiogenesis, and resulted in altered cell morphology (King et al., 2014). Finally, nesprin-3 has been shown to be required for flow-induced polarization of the centrosome and flow-induced migration (Morgan et al., 2011). Collectively these data indicate that the connection of the cytoskeleton to the nucleus is of critical importance to endothelial cells.

To build on this prior work examining the LINC complex in endothelial cells, our group utilized a dominant negative KASH (DN-KASH) peptide that has been previously shown to disrupt endogenous nesprin protein localization at the nuclear envelope (Lombardi et al., 2011; Zhang et al., 2019). Additionally, this dominant negative approach has the added advantage that all nesprins are displaced, whereas knockdown of individual nesprins could result in compensation by other nesprin isoforms. When expressed in HUVEC, this resulted in endothelial cells with nuclei decoupled from the actin, microtubule, and intermediate cytoskeletons. Expression of DN-KASH in HUVEC resulted in endothelial cells with defective barrier function, impaired cell spreading and adhesion, and defects in migration, angiogenesis, and adaptation to fluid shear stress.

RESULTS

Disruption of the LINC complex impairs endothelial barrier

To completely disrupt the LINC complex, we utilized a previously characterized dominant negative peptide, known as DN-KASH, in which overexpression of this peptide saturates available binding sites on SUN proteins and displaces endogenous nesprin isoforms from the nuclear envelope (Lombardi et al., 2011). mCherry-tagged dominant negative KASH (the KASH domain of nesprin-1) was expressed in HUVEC using adenovirus. To control for the effects of adenoviral infection, the effects of mCherry DN-KASH were compared with cells exposed to mCherry adenovirus. As expected, mCherry DN-KASH expression resulted in loss of nesprin-1 and nesprin-2 localization on the nuclear envelope, indicating LINC complex disruption, whereas expression of mCherry alone had no effect on nesprin localization to the nuclear envelope (Figure 1A). As a further control to account for any potential effects of overexpression of a partial nesprin protein, we expressed a previously developed mutated DN-KASH, mCherry-KASH1ΔPPPL (abbreviated as PPPL), in which the last four amino acids (PPPL) were removed (Zhang et al., 2019). The PPPL construct retains similar localization to DN-KASH but is unable to disrupt endogenous nesprin proteins from the nuclear envelope (Supplemental Figure S1A).

Untransduced or mCherry control expressing HUVEC, seeded at confluency and fixed 2 d later, quickly formed and maintained a confluent monolayer with well-formed cell-cell contacts. In contrast, endothelial cells expressing DN-KASH had reduced confluency, as well as noticeable gaps between cells (Figure 1B), indicating that DN-KASH affects endothelial monolayer formation and/or barrier integrity. We decided to look at barrier integrity by using an electrical impedance assay (Xcelligence; Roche), to examine the kinetics of barrier formation for endothelial cells expressing mCherry or DN-KASH. In this experiment we seeded cells already expressing DN-KASH or mCherry on the Xcelligence system electrodes and acquired impedance for 24 h. No differences were observed in the first 6 h. After this time both nontransduced cells and mCherry control cells exhibited a linear increase in impedance, indicating the formation of a barrier. In contrast, DN-KASH-expressing cells do not reach as high of an impedance, suggesting either cell detachment or reduced barrier function (Figure 1C). As an additional control for the potential effect of adenoviral infection, a tetracycline-driven mCherry DN-KASH adenovirus was used in which DN-KASH expression can be induced with doxycycline (dx). Induction of DN-KASH expression significantly affected barrier formation in cells compared with noninduced infected cells (Figure 1C). Additionally, endothelial monolayer integrity was further examined using a fluorescence permeability assay (Dextran-FITC 70 kDa). The coefficient of permeability was higher for DN-KASH cells as compared with nontransduced cells and mCherry cells (Figure 1D). Together, these results illustrate that disruption of the LINC complex has a significant impact on the formation and stability of endothelial cell monolayers with regard to cell-cell adhesion and barrier function.

Disruption of the LINC complex affects endothelial cell adhesion

Because we observed reduced cell confluence in DN-KASH-expressing endothelial cells (Figure 1B), we sought to understand whether there were any cell-matrix or cell-cell adhesion defects in LINC-disrupted HUVEC. First, we measured the electrical impedance of cells during the first hour of attachment and observed no differences between DN-KASH-expressing and mCherry control cells (Figure 2A), suggesting that LINC complex disruption does not prevent initial cell attachment to the substrate. Next, we examined whether DN-KASH affected later-stage adhesion (e.g., firm adhesion) by examining cellular attachment rates by seeding identical numbers of cells on slides, followed by rinsing in phosphatebuffered saline (PBS) and then fixation. DN-KASH-expressing cells exhibited an approximate 50% (0.55 \pm 0.08 at 30 min, 0.56 \pm 0.26 at 60 min) reduction in attachment (Figure 2B), indicating that cells are more readily displaced under the mechanical forces of rising, suggesting weaker cell-extracellular matrix (ECM) adhesion. Indeed, live cell imaging of cell adhesion showed that DN-KASH expression reduced adhesion and spreading over 24 h (Figure 2C; Supplemental Movie S1). As a further mechanical challenge, we examined the effects of stretch on both cell-cell adhesion and cell-ECM adhesion. To assay cell-cell adhesion we coexpressed an existing VE-cadherin Förster resonance energy transfer (FRET) force tension sensor (Conway et al., 2013) in endothelial cells expressing DN-KASH or mCherry control. DN-KASH-expressing unstretched cells (0% strain) had significantly increased VE-cadherin FRET (indicating reduced tension) compared with unstretched (0%) mCherry control cells (Figure 2D). When these cells were exposed to 15% radial stretch, VE-cadherin in mCherry control cells exhibited a relaxation in response to 15% radial stretch (0.324 \pm 0.092 to 0.368 \pm 0.093), whereas cells expressing DN-KASH exhibited reduced force across VE-cadherin with no change in tension in response to stretch (0.396 \pm 0.070 to 0.380 \pm 0.085) (Figure 2D). Therefore DN-KASHexpressing cells appear to have adherens junctions in an altered

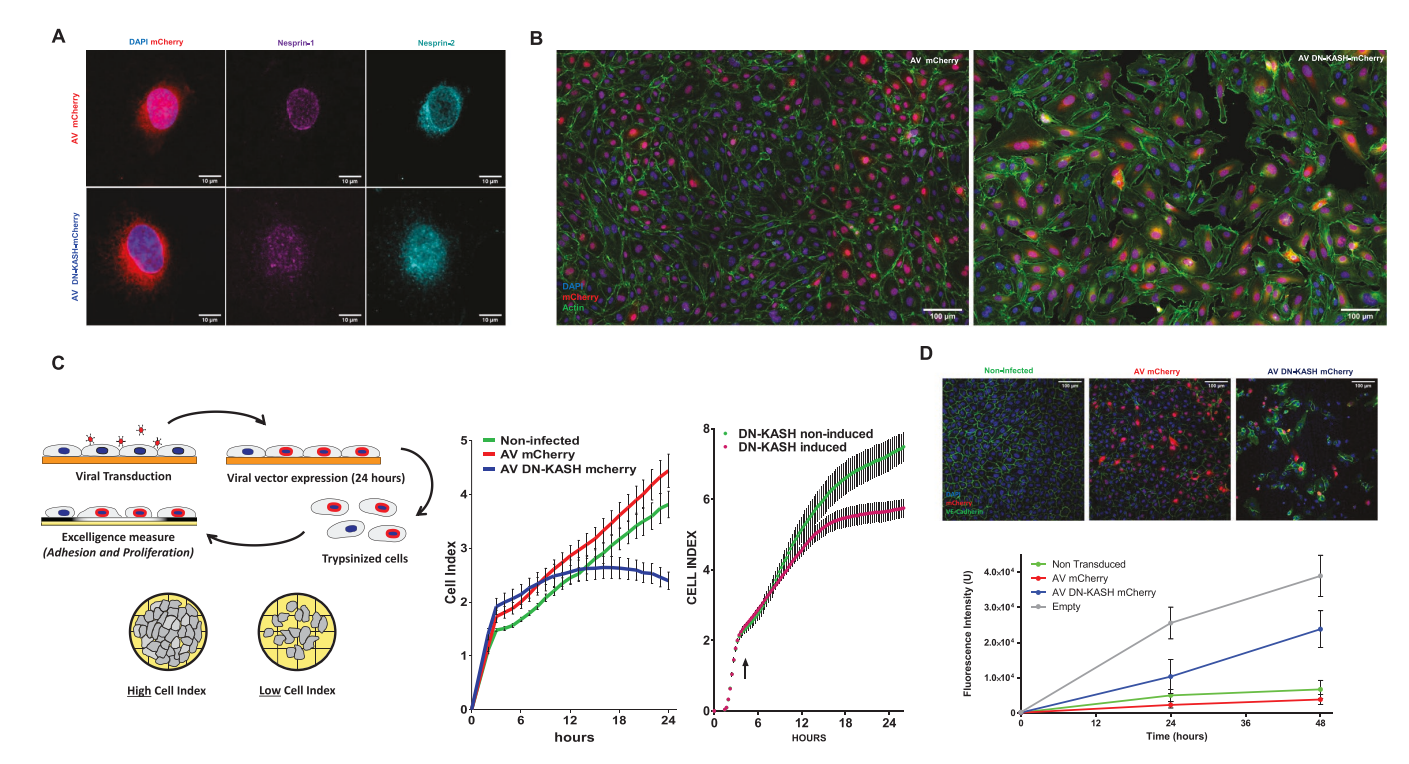


FIGURE 1: DN-KASH expression disrupts the LINC complex and affects barrier formation. (A) Cells expressing adenovirus (AV) mCherry (red) or DN-KASH mCherry (red) were stained for nesprin-1 (magenta) and nesprin-2 (cyan). (B) Immunofluorescence of HUVEC-expressing mCherry adenovirus or DN-KASH-mCherry adenovirus after 48 h of growth. Cells were stained for DAPI (blue), actin (green), and mCherry (red). (C) Electrical impedance was measured for HUVEC infected by mCherry adenovirus (red) or DN-KASH-mCherry (blue) or noninfected control (green). HUVEC were seeded on Xcelligence plate (Roche) and impedance recorded over time (cell index). In a separate experiment, impedance was also measured for HUVEC infected by inducible DN-KASH-mCherry adenovirus. At 5 h, DN-KASH is induced with doxycycline (DN-KASH TetON) or left uninduced (DN-KASH TetOFF). Each condition is recorded for four different wells; error bars represent SE. Representative curves of three independent experiments. Representative images of three independent experiments. (D) Permissibility to Dextran-FITC 70 kDa was assessed for HUVEC infected by adenovirus-mCherry or DN-KASH-mCherry on 0.4 µm Transwells. After 12 h, Dextran-FITC 70 kDa is added to the apical surface of cells. This point represents time 0 h. Basal fluorescence was measured 24 and 48 h later. After fixation, cells on Transwells were immunostained with DAPI and VE-cadherin antibody.

mechanical state (reduced force), with impaired responses to application of mechanical force. Although stretch is often expected to increase protein forces, including across epithelial cell-cell junctions (Borghi et al., 2012), we note that endothelial cells have been shown to actively relax in response to externally applied forces, which occur as part of an active signaling mechanism (Conway et al., 2013, 2017). Finally, we observed that DN-KASH cells subjected to constant 15% stretch detached over a time period of 60 min, whereas control cells remained adhered (Figure 2E; Supplemental Movie S2). In summary, the LINC complex appears to be necessary for cell adhesion and adaptation against mechanical stress.

Disruption of the LINC complex affects focal adhesion dynamics

Cell adaptation to mechanical forces likely involves changes in focal adhesion dynamics, including focal adhesion remodeling. Therefore, we examined how LINC complex disruption affected focal adhesion dynamics. First, we observed differences in vinculin distribution during cell spreading after 30 min of adhesion. Control cell–expressing mCherry showed a characteristic focal adhesion profile, organized in focal structures oriented toward the cell center (Figure 3A). In contrast, DN-KASH–expressing cells showed fewer

focal adhesions, which were primarily distributed at the cell edge, without specific orientation (Figure 3A). In addition, actin organization was also be impaired in DN-KASH-expressing cells, with increased actin at cell edges and reduced stress fibers visible throughout the cell as compared with mCherry control cells (Figure 3A). Additionally, we observed altered organization of the vimentin intermediate filament network in these cells (Figure 3B). Vimentin fibers are evenly distributed throughout the entire cell in the mCherry control cells, whereas there is a collapse of the vimentin filament network around the nucleus in DN-KASH-expressing cells. This vimentin network organization is not visible with a PPPL mutant (Supplemental Figure S1B). To examine whether the altered focal adhesions in DN-KASH-expressing cells affected the forces across focal adhesion proteins, we used an existing vinculin FRET tension sensor (Grashoff et al., 2010) to measure vinculin forces in cells that had adhered for 12 h. We observed only a slight difference in FRET for control cells expressing mCherry vector (0.42 \pm 0.12) as compared with vinculin TSmod FRET in DN-KASH-expressing cells (0.40 \pm 0.10) (Figure 3C). The observation of a similar vinculin mechanical loading between DN-KASH and mCherry cells indicates that the focal adhesions in DN-KASH cells are connected to actin and experiencing mechanical tension. Finally, we investigated whether focal adhesion signaling is altered by LINC complex disruption. We

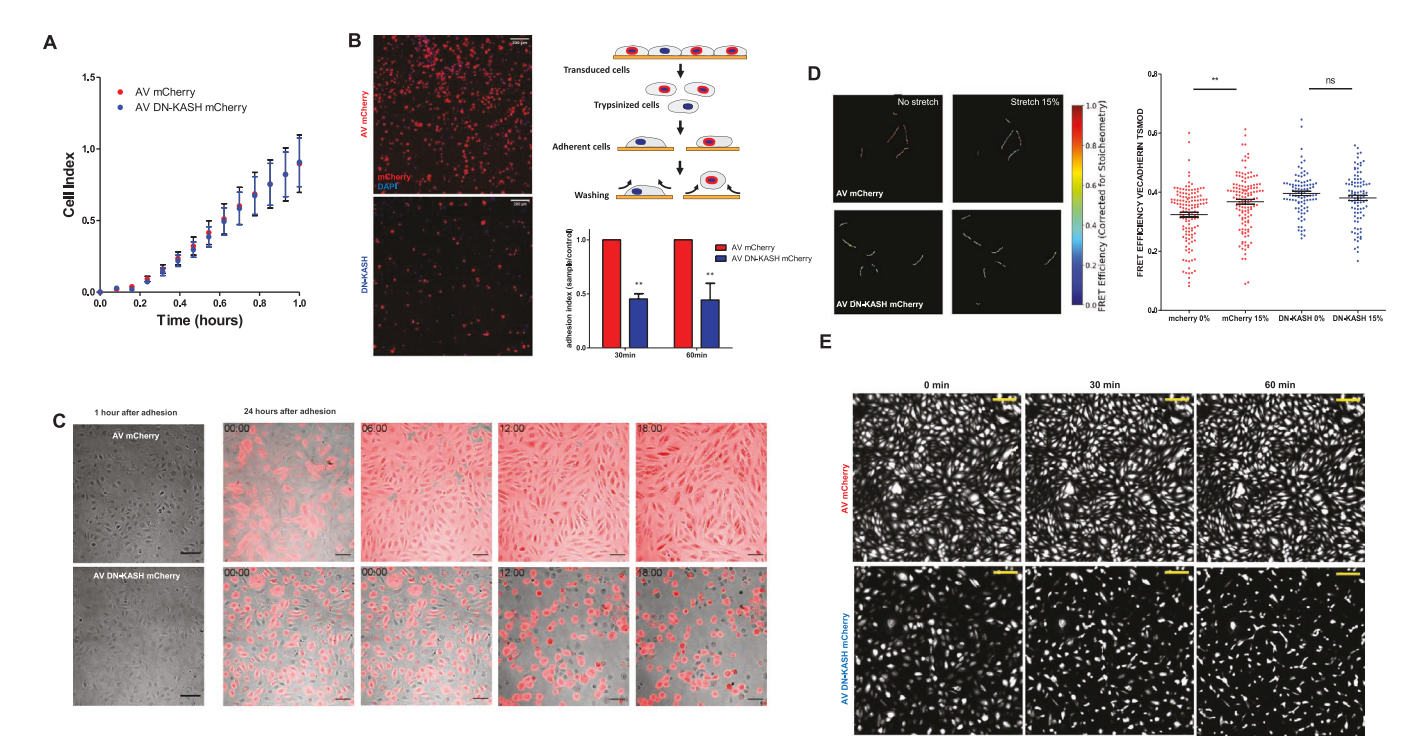


FIGURE 2: Disruption of the LINC complex affects endothelial cell-cell adhesion. (A) Ten thousand HUVEC were seeded on Xcelligence plate (Roche) and impedance recorded over time (cell index). HUVEC infected by mCherry adenovirus (red) or DN-KASH-mCherry (blue) were measured for electrical impedance over 1 h. Representative curves of three independent experiments. (B) HUVEC, already expressing DN-KASH, were trypsinized, counted, and seeded onto fibronectin-coated surfaces. One hundred thousand cells were allowed to adhere for 30 or 60 min before being washed with PBS and then paraformaldehyde fixation. Cells were imaged, and the quantification was performed using ImageJ N = 3, Two-way ANOVA (** p < 0.01). (C) Live microscopy of HUVEC. Cells were seeded onto a fibronectincoated glass dish and transduced with AV mCherry or AV DN-KASH-mCherry. A field was acquired 1 h after adhesion and live-time acquisition started 24 h later on the same field. (D) HUVEC were coinfected by adenovirus-mCherry or DN-KASH-mCherry with VE-cadherin tension-sensor adenovirus. Cells were seeded onto PDMS membrane coated with fibronectin and mounted on the Isostretcher stretching device. The same junctions are acquired before (no stretch) and after 15% PDMS membrane stretch (stretch 15%). N = 3, Mann–Whitney test (** p < 0.01). (E) HUVEC were infected by adenovirus-mCherry or DN-KASH-mCherry. Cells were seeded on PDMS membrane coated with fibronectin and mounted on the Isostretcher stretching device. After 24 h, PDMS membrane was stretched at a constant 15% strain with a time lapse imaging over 1 h.

observed decreased pY1065 vinculin, decreased pY397 FAK, and increased pS425 talin in DN-KASH spreading cells (Figure 3D), whereas PPPL mutant-expressing cells had normal focal adhesion phosphorylation profiles (Supplemental Figure S1C). Taken together, our results indicate dramatically altered signaling in focal adhesions, which may affect adhesion strength and adaptation to mechanical challenge.

Effects of LINC complex disruption on cell proliferation

Because of the observed defects in cell-cell adhesion and focal adhesion formation, we hypothesized that disruption of the LINC complex could also impact endothelial cell proliferation. Indeed DN-KASH-expressing cells seeded at subconfluency exhibited the slowest growth rate as compared with PPPL, mCherry, or untransfected controls (Supplemental Figure S2A). Interestingly, Ki67 staining and EdU incorporation were enhanced in DN-KASH cells (Supplemental Figure S2B). These data indicate that LINC complex disruption does not block entry into the cell cycle (Ki67-positive cells) or DNA replication (EdU incorporation), but rather instead affects some other critical aspect of later-stage cell division, such as mitosis.

The nuclear LINC complex is required for endothelial adaptation to physiological forces, wound healing, and angiogenesis

On the basis of our results, we hypothesized that the impaired adhesion and barrier function of endothelial cells would render LINC complex-disrupted cells unable to adapt to physiological forces. First, we examined the response of these cells to low shear stress (6 dynes/cm²). Cells expressing DN-KASH detached after 24 h of low levels of shear stress, whereas control cells (noninfected, mCherry, or PPPL expressing) remained attached (Figure 4A and Supplemental Figure S3A). Cells expressing inducible DN-KASH adenovirus also exhibit flow-induced cell detachment only when DN-KASH was induced with doxycycline (Supplemental Figure S3B). Next, endothelial cells were exposed to normal arterial levels of shear stress (12 dynes/cm²) for 24 h. Noninfected cells do not completely align after 24 h of shear stress (but do align at longer time periods; unpublished data). Interestingly, mCherry-expressing endothelial cells aligned after 24 h of arterial shear stress, which may be a function of increased inflammation from adenoviral infection. DN-KASH-expressing cells also aligned (as indicated by cell elongation in the direction of flow) but also exhibited significant cell detachment

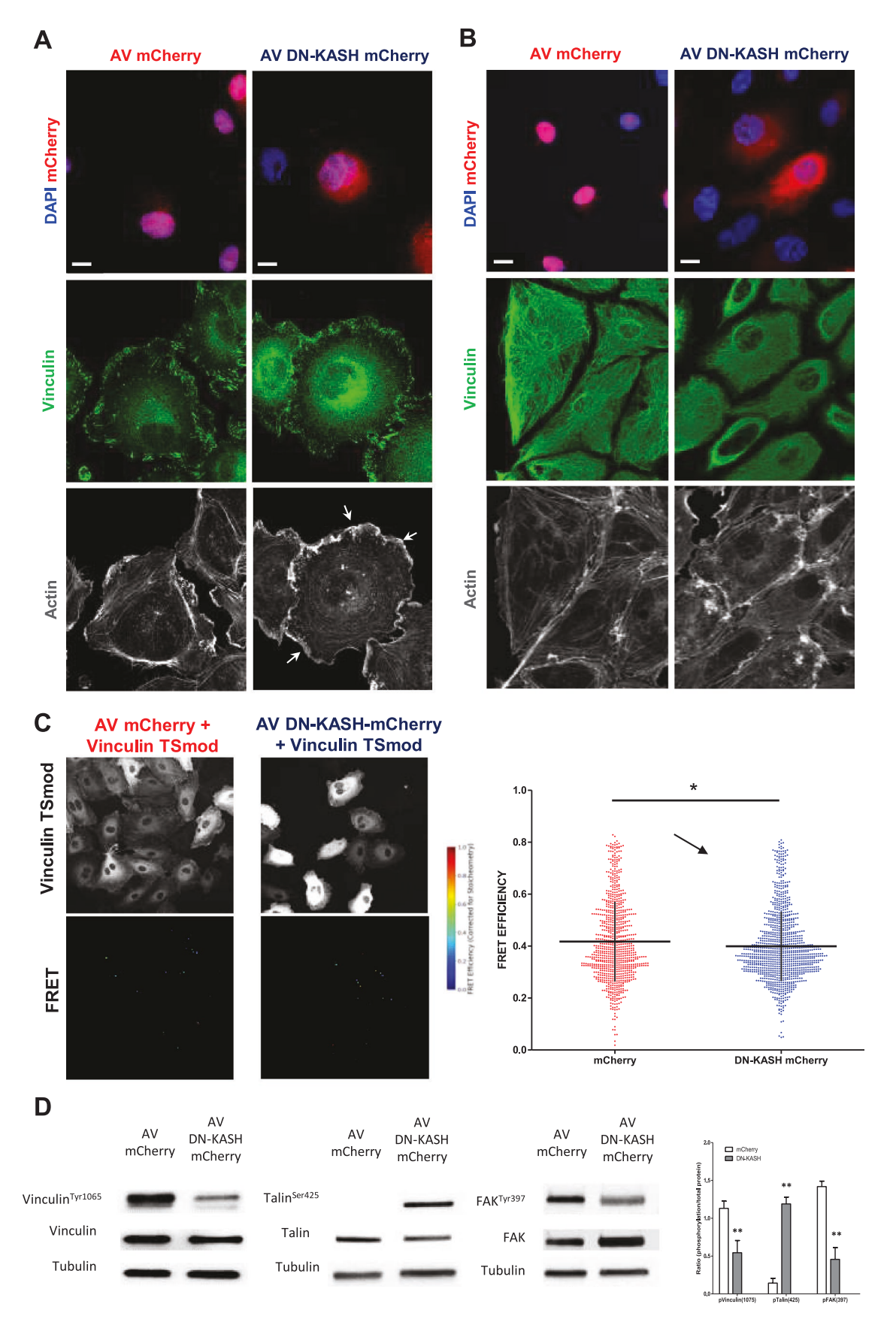


FIGURE 3: Disruption of the LINC complex affects focal adhesion dynamics. (A) DN-KASH affects focal adhesion morphology. Cells expressing AV-mCherry or AV-DN-KASH-mCherry were immunostained for DAPI, vinculin, or vimentin (green) and actin (gray). (B) DN-KASH expression affects the vimentin cytoskeleton. Cells expressing AV-mCherry or DN-KASH-mCherry were immunostained for DAPI, vimentin (green), and actin (gray). (C) Cells were cotransfected with

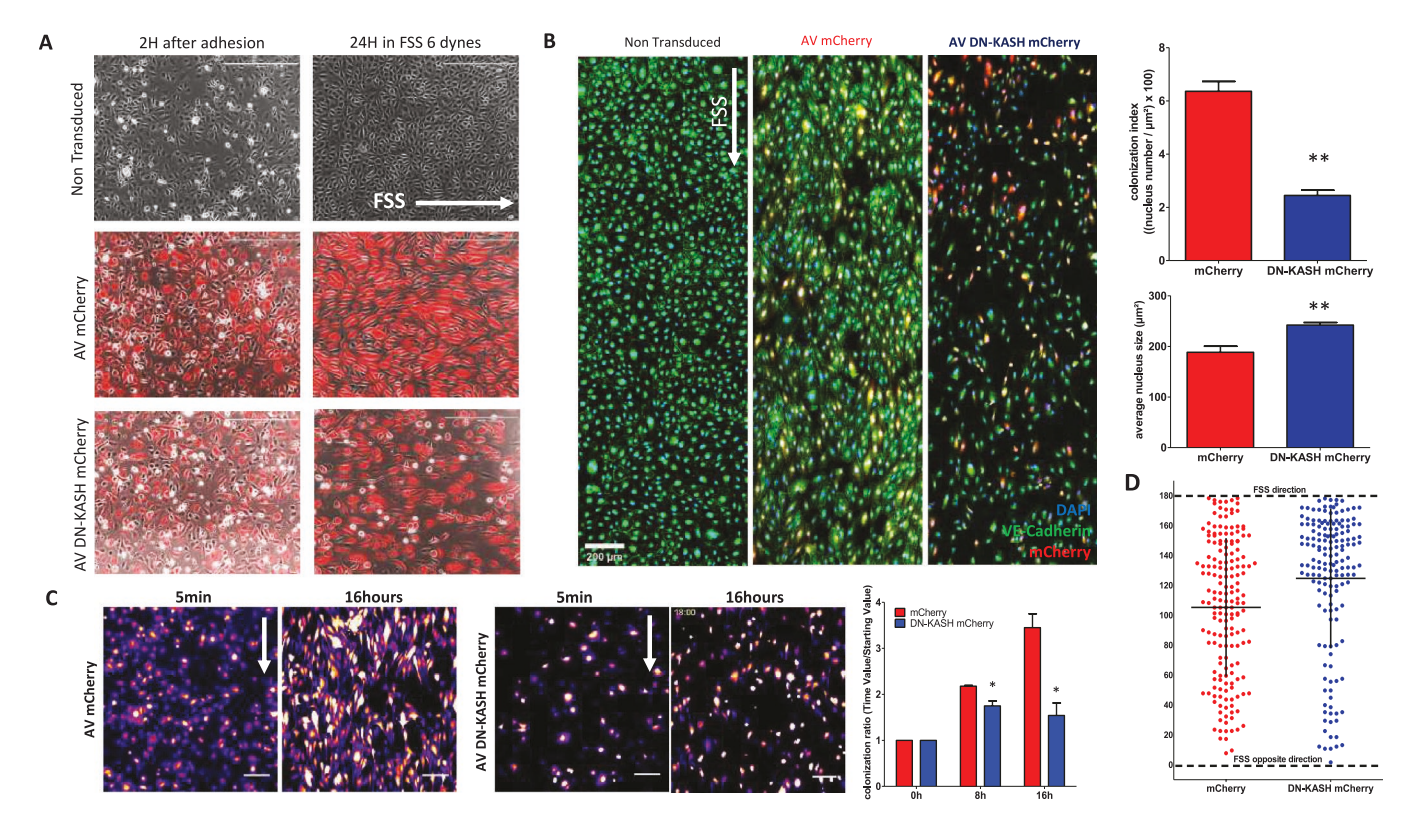


FIGURE 4: Disruption of the LINC complex prevents endothelial adaptation to physiological forces, wound healing, and angiogenesis. (A) LINC complex disruption results in cell detachment at low levels of shear stress. HUVEC-expressing AV DN-KASH or AV-mCherry control were seeded in IbidiTreat channels 2 h before flow stimulation (high cell density—100,000 cells/channel). Shear stress was applied for 24 h at 6 dynes/cm². (B) Fluid shear stress at arterial levels of shear stress results in increased detachment of LINC complex—disrupted cells. HUVEC were seeded in IbidiTreat channels 24 h before flow stimulation (70,000/channel) and then exposed to 24 h of 12 dynes/cm² shear stress. To quantitate the number of cells, a colonization index was measured (number of nuclei per micron²). Additionally, the size of the nucleus was increased in DN-KASH—expressing cells. Mann-Whitney test (** p < 0.01). (C) Live cell imaging of cells expressing mCherry-DN-KASH or mCherry control showed that cell detachment of LINC complex—disrupted cells happens early (<6 h). Number of fluorescent cells in the channel is quantified. Ratio is obtained by 0 h/x h. Two-way ANOVA (* p < 0.05). (D) Quantification of nucleus-pericentrin orientation of cells expressing mCherry control or DN-KASH after exposure to fluid shear stress. N = 3, Mann—Whitney test (** p < 0.01).

(mCherry control 6.4 ± 1.7 cells/ μ m², DN-KASH 2.4 ± 0.9 cells/ μ m²). In addition, we observed that the nucleus size of adherent DN-KASH cells is larger compared with that of mCherry control (control 188.3 ± 12.0 pixels, DN-KASH 242.2 ± 5.0 pixels) (Figure 4B). To validate these observations, we tracked endothelial cells under reduced levels of shear stress (6 dynes/cm²) over 16 h. We observed that DN-KASH–expressing cells are not able to expand across the substrate to become confluent, and instead roll, detaching rapidly, with some instances of upstream migration (Figure 4C; Supplemental Movie S3). We analyzed the orientation of the nucleus–pericentrin axis of cells exposed to 12 dynes/cm² shear stress for 24 h. Cells expressing DN-KASH were more aligned in the direction of flow (AV-mCherry, 105.3 ± 3.4 , N=178 and AV-DN-KASH, 124.7 ± 3.6 , N=162) (Figure 4D).

Next, we examined how LINC complex disruption affected wound healing and tubulogenesis. In a wound healing assay, the migration speed of endothelial cells expressing DN-KASH was not slower during the first few hours of wound closure than that of mCherry-expressing and uninfected control cells. However, later time points showed that DN-KASH-expressing cells were unable to close a wound in the late phase (Figure 5A). PPPL-expressing cells still possess the ability to close a wound, which illustrates that it is the disruption of the LINC complex that it is responsible for this phenotype (Supplemental Figure S4A). It is notable that the collective migration of DN-KASH-expressing cells seems to be impacted. Indeed, migration of mCherry control cells is organized into the direction of empty space, where DN-KASH-expressing cells show a "chaotic" migration associated with a cell-cell detachment

vinculin-TSmod and AV-mCherry or DN-KASH-mCherry. Force exerted across vinculin is reduced upon LINC disruption in HUVEC. Coinfected cells with adenovirus-mCherry or DN-KASH-mCherry with vinculin tension-sensor (TSmod). Mann–Whitney test (* p < 0.05), N = 3. (D) Altered phosphorylation states of focal adhesion proteins with DN-KASH expression. HUVEC-expressing AV-DN-KASH or AV-mCherry control were lysed for 36–48 h and blotted for pY1065 vinculin, pS425 Talin, and pY397 FAK (N = 3). Mann–Whitney test (** p < 0.01).

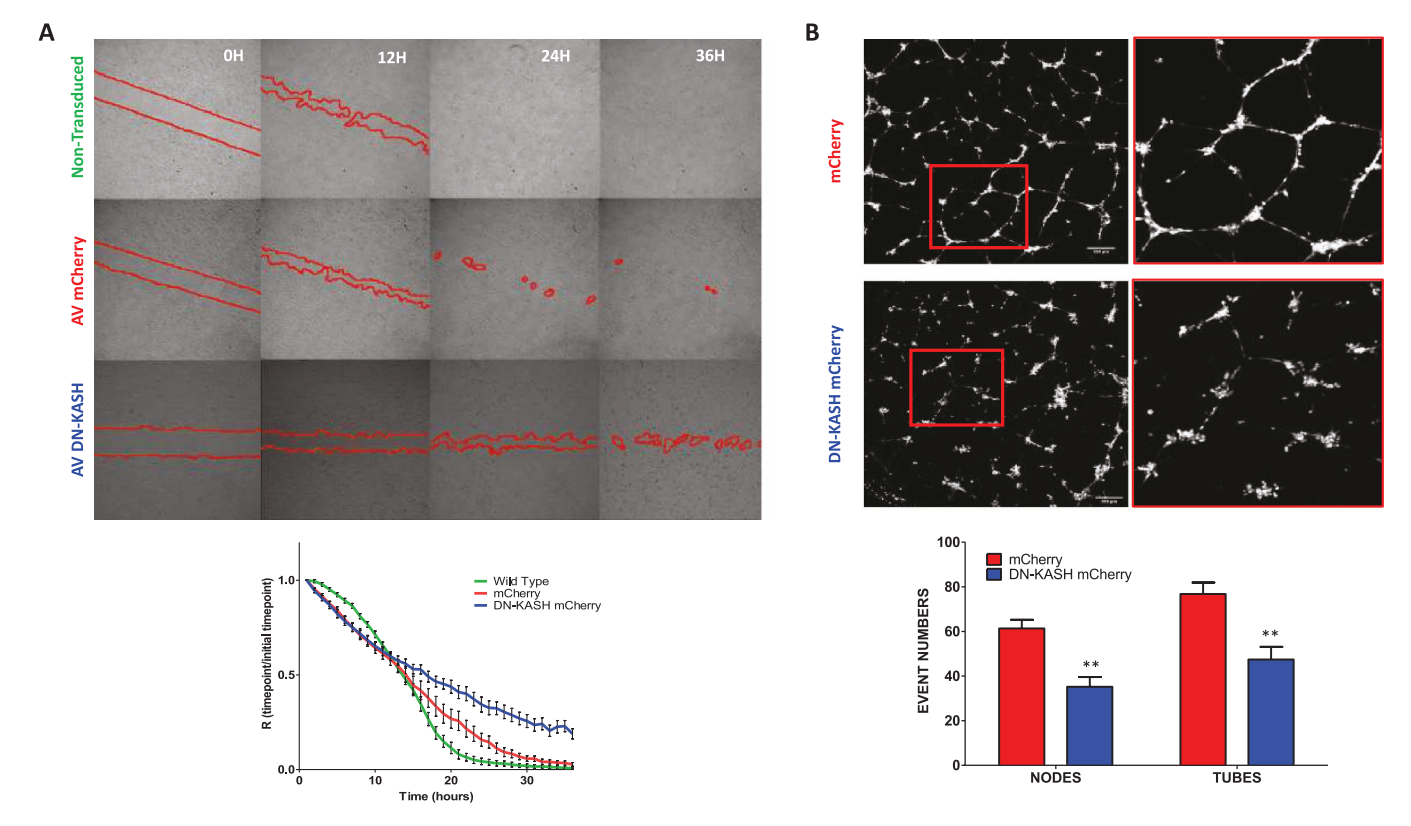


FIGURE 5: Disruption of LINC complex alters wound healing and angiogenesis. (A) LINC complex–disrupted endothelial cells have delayed wound healing in a scratch wound assay. Fifty thousand cells were seeded in the Culture-Insert 4 Well in an μ -Dish from Ibidi and infected by AV-mCherry or AV-DN-KASH-mCherry for 24 h. The insert was removed, cells were washed, and acquisition started. Ratio of T+1/T0 was done to visualize wound healing closing from three independent experiments. (B) LINC complex–disrupted endothelial cells have impaired sprouting in an in vitro angiogenesis assay. Representative fields of 3 independent experiments. Cells infected by Adenovirus mCherry (AV mCherry) or Adenovirus DN-KASH mCherry (AV DN-KASH). Mann-Whitney test (** p < 0.01).

(Supplemental Figure S4B; Supplemental Movies 4 and 5). We also examined angiogenesis potency by examination of endothelial tube formation. Endothelial cells expressing DN-KASH had reduced nodes and tubes formed compared with control condition (control 61.3 \pm 9.0 nodes and 76.8 \pm 11.6 tubes per field, DN-KASH 35.2 \pm 10.8 nodes and 47.4 \pm 14.1 tubes per field) (Figure 5B). Together, these results demonstrate that LINC complex disruption impacts fundamental endothelial-specific processes, including the adaptation to shear stress, wound closure, and three-dimensional tube formation.

DISCUSSION

In this article we sought to examine the importance of the LINC complex in endothelial cell function and adaptation to externally applied forces by using a dominant negative KASH peptide to disrupt the LINC complex. In previous studies small interfering RNA knockdown of individual nesprin isoforms demonstrated important roles of nesprin-1, nesprin-2, and nesprin-3 in endothelial cells (Chancellor et al., 2010; Morgan et al., 2011; Anno et al., 2012; King et al., 2014). We note that DN-KASH expression elicits more severe phenotypes (cell detachment and impaired focal adhesion dynamics) than knockdown of individual isoforms, suggesting possible redundancy or compensation between nesprin isoforms. Importantly, expression of a control DN-KASH, Δ PPPL, which is unable to bind endogenous SUN proteins and disrupt endogenous nesprin binding to the nucleus, did not have major effects on endothelial cell attachment, focal adhesions, or wound healing, indicat-

ing that it is the physical disruption of nuclear-cytoskeletal connections that is responsible for the phenotypes observed with DN-KASH expression.

A major function of the endothelium is to provide barrier function. Interestingly impaired barrier function was observed for cells in which the LINC complex was disrupted (Figure 1), suggesting a relationship between cell-cell adhesion and the LINC complex. Work by Megan King's group has shown a similar disruption of cell-cell adhesion in keratinocytes deficient in SUN2 (Stewart et al., 2015), suggesting that the LINC complex may play an important role in cell-cell adhesion and barrier function in different cell types. In endothelial cells we observed that LINC complex disruption also reduced resting VE-cadherin tension (Figure 2D), suggesting that the adherens junction may be mechanically compromised. Because LINC complex disruption also reduced cell proliferation (Supplemental Figure S2) and increases cell detachment (Figures 2 and 4), it is likely that the impaired barrier function observed in Figure 1 results from a combination of reduced cell proliferation, increased cell detachment, and impaired cell-cell adhesions.

DN-KASH–expressing cells have delayed migration in a wound healing assay (Figure 5; Supplemental Figure S4). Similar delayed migration was observed for endothelial cells depleted of either nesprin-1 or nesprin-2 (King et al., 2014). Additional studies have shown delayed migration in LINC-disrupted fibroblasts (Luxton et al., 2010; Lombardi et al., 2011; Woychek and Jones, 2019). One notable observation in our movies of the wound healing assay was that the migratory behavior of DN-KASH–expressing cells was more

"chaotic" (Supplemental Movies 4 and 5), which may be indicative that disruption of the LINC complex causes a switch from collective cell migration to single cell migration. Indeed, disruption of the LINC complex in *Drosophila* inhibited epithelial collective migration (Myat et al., 2015). Because mechanical tension across cell-cell adhesions is thought to be an important component in collective migration (Trepat et al., 2009), it is possible that the reduced VE-cadherin forces (Figure 2D) in DN-KASH cells impair collective migration. Additionally we note recent work by the Kris Dahl group that has shown that DN-KASH expression in a single cell affects the cellular forces in nearby cells (Armiger et al., 2018), showing that the LINC complex is important for propagation of force between cells across a monolayer.

In addition to barrier function, the endothelium is unique for the types of physiological forces it is required to adapt to and withstand. Blood vessels are exposed to fluid shear stress (frictional drag of blood flow) and cyclic stretch (caused by the pulsatility of blood flow). We observed that the LINC complex is required to adapt to the mechanical forces of fluid shear stress (Figure 4, A-C) and cyclic stretch (Figure 2E). Cells with LINC complex disruption were observed to detach when exposed to fluid shear stress and cyclic stretch, suggesting that there is impaired cell adhesion to the ECM. Prior work has shown that DN-KASH expression reduces perinuclear focal adhesion forces in fibroblasts (Shiu et al., 2018). Interestingly, we also observed altered focal adhesion morphology as well as a dysregulation of focal signaling phosphorylation for cells expressing DN-KASH (Figure 3). Changes in the phosphorylation state of vinculin, talin, and FAK suggest that the LINC complex is important for focal adhesion signaling and adaptation in response to changes in mechanical force. Of note, a prior study showed that inhibition of phosphorylation of Y1065 of vinculin leads to an uncontrolled exchange of vinculin and reduced cell adhesive forces (Küpper et al., 2010), suggesting that the change in phosphorylation state of focal adhesion proteins observed in endothelial cells expressing DN-KASH is indicative of impaired focal adhesion dynamics and reduced adhesivity. In addition, two recent studies have shown that loss of nesprin-1 (Nguyen et al., 2019) or nesprin-2G (Woychek and Jones, 2019) negatively affects cell migration, further suggesting a relationship between the LINC complex and cell-matrix adhesion (Nguyen et al., 2019), potentially through direct cytoskeleton force transmission between these two regions of the cell. Notably, one of these studies showed that loss of nesprin-1 affected ERK and FAK signaling (Nguyen et al., 2019).

In summary, our work in this article further identifies the importance of the LINC complex in cellular homeostasis, highlighting the cross-talk between the LINC complex, cell-cell junctions, and cellmatrix adhesions. The LINC complex, and by extension the entire nucleus, has long been thought of as a potential mechanotransducer of force, converting physical forces into changes in gene expression (Dahl et al., 2008; Wang et al., 2009). Our work shows that in addition to serving as a mechanotransducer of force, the LINC complex is a fundamental physical structure that is required for the mechanical stability of the endothelium. Given that LINC complex disruption in other cell types (fibroblasts, epithelium) results in less severe phenotypes, it will be interesting to learn the reasons why the LINC complex is especially critical in endothelial cells, including whether this is related to the enhanced mechanosensitivity and mechanoadapation of the endothelium.

MATERIALS AND METHODS

Request a protocol through Bio-protocol.

Cell lines and reagents

Human umbilical vein endothelial cells (HUVEC) were purchased from Promocell (C-12250) and were grown in associated media EGM-2 (C-22011) from Promocell without antibiotics. A list of the antibodies used in this work is shown below. Far red phalloidin (Acti-Stain 670) was purchased from Cytoskeleton and 4',6-diamidino-2-phenylindole (DAPI) from ThermoFisher. For regular immunofluorescence, cells were seeded and stained on Ibidi μ-slide eight wells (80826) or poly-lysine glass coverslip coated with bovine fibronectin 25 µg/ml (Sigma F1141) or porcine gelatin 2% (Millipore 48724).

Antibodies used: Anti-nesprin-1: Mouse monoclonal, clone MANNES1A, Catalogue #: MA5-18077, ThermoFisher; Anti-nesprin-2: Rabbit polyclonal, gift of Gregg Gundersen, Columbia University (Luxton et al., 2010); Anti-VE-cadherin: Mouse monoclonal, clone#123413, Catalogue #: MAB9381, R&D Systems; Anti-vinculin: Rabbit monoclonal, clone EPR8185, Catalogue #: ab129002, Abcam; Anti-vimentin: mouse monoclonal E-5, Catalogue #: sc-373717, Santa Cruz; Anti-vinculin (PhosphoTyr1065): Rabbit polyclonal, Catalogue #: 44-1078G, ThermoFisher; Anti-talin: Mouse monoclonal, clone 8d4, Catalogue # : T3287, Sigma; Anti-talin (PhosphoSer425): Rabbit polyclonal, Catalogue # 5426, Cell Signaling; Anti-Fak: Rabbit polyclonal, Catalog #: 3285, Cell Signaling; Anti-Fak (PhosphoTyr397): Rabbit polyclonal, Catalogue #: 3283, Cell Signaling; Anti-Ki-67: Rabbit polyclonal, Catalogue #: PA5-19462, ThermoFisher Scientific.

For EdU labeling, the ClickiT EdU Alexa Fluor 647 Imaging Kit (ThermoFisher; C10340) was used according to the manufacturer instructions.

Plasmids and adenovirus

DN-KASH is a previously used dominant negative protein consisting of the KASH domain of nesprin (C-terminus of the protein, including the transmembrane domain) (Mayer et al., 2019; Zhang et al., 2019). In these studies we coupled mCherry with the KASH domain of nesprin-1 (consisting of both the transmembrane domain of nesprin-1 and the KASH domain of nesprin-1) to form mCherry-DN-KASH (Addgene plasmid 125553). DN-KASHΔPPPL (Addgene plasmid 129280), lacking the last four amino acids (PPPL) of the KASH domain and unable to disrupt endogenous nesprins, was used as a control (Zhang et al., 2019). The design of VE-cadherin TSmod (Conway et al., 2013) (Addgene plasmid 45848) and vinculin TSmod (Grashoff et al., 2010) (Addgene plasmid 26019) were previously described. The cDNA sequences for DN-KASH and VE-cadherin TSmod were subcloned into pShuttleCMV (Addgene plasmid 16405) and then recombined into pAdEasy-1 (Addgene plasmid 16400), following the AdEasy Adenoviral Vector System instructions (Agilent). Vinculin TSmod and DN-KASHΔPPPL were cloned into donor vectors, followed by Gateway insertion into the pAd/CMV/V5-DEST Gateway Vector (ThermoFisher). Adenovirus was made using 293A cells, per manufacturer instructions. Control adenovirus (expressing mCherry) was purchased from Vector Biolabs (Catalogue #1767). A tetracycline-inducible mCherry DN-KASH adenovirus was made using the Adeno-X Adenoviral System 3 (Tet-On 3G Inducible) system (Takara Bio USA) per manufacturer instructions.

Impedance assay

Impedance of the HUVEC monolayer was performed on Xcelligence system (ACEA Biosciences). Cells are transduced 16 h before the experiment in a six-well plate. Then, 10,000 cells (noninfected, AV mCherry, and AV DN-KASH) or 20,000 cells (DN-KASH inducible) were seeded on ACEA 96-well plates coated with gelatin 2%. A period of 15 min at room temperature was necessary to let cells adhere. The number of cells to reach the plateau in 3 days was determined, and impedance acquisition was done every 15 min until the end of the experiment. Values were extracted from RCTA software and analyzed by Prism.

Permeability assay

Endothelial cells were seeded at high density on Transwells (Corning CLS3391; 0.4 μ m) and transduced with adenovirus 24 h before the starting point of the experiment. The next day EBM2 media containing Dextran-FITC (fluorescein isothiocyanate) 70 kDa (Sigma 46945) was added in the top well. Measurements started at this time point by collecting 10 μ l in the bottom well. FITC fluorescence was measured using the Synergy H1 Hybrid Reader (Biotek).

Stretch experiment

An automated radial stretcher (IsoStretcher [Schürmann et al., 2016]) was used to apply stretch. Cells were seeded on PDMS stretcher wells coated with fibronectin (25 μ g/ml) and allowed to adhere overnight. Mechanical stretch was applied to the polydimethylsiloxane (PDMS) membrane step-by-step (1% every 10 s) to reach 15% stretch. The stretch experiment was performed in a temperature- and CO₂-controlled incubator during the acquisition on LSM 700.

Fluid shear stress experiments

Cells were seeded on Ibidi slides with one or six channels Ibiditreat $\mu\text{-Slide}$ I Luer 0.4 mm (Ibidi 80176 or 80606). Slides containing cells were incubated at 37°C 5% CO $_2$ without shear stress during a minimal time of 2 h, depending on the experiment. $\mu\text{-Slides}$ were connected to an Ibidi pump system (10902) and 6 dynes/cm² shear stress was applied for 2 h before 12 dynes/cm² shear stress was applied for 24 h. For live cell imaging of cells under shear stress, cells were seeded and transduced overnight in an Ibidi channel. Shear stress was applied at 12 dynes/cm². For time-lapse imaging experiments, images were captured every 30 min for 12 h using a Nikon Eclipse Ti2.

Wound healing assay

Cells were seeded and transduced by adenovirus in an Ibidi microinsert IbidiTreat culture dish (81176). After an overnight incubation, cells were washed and the insert was removed. The acquisition started at this time point, on a Nikon Eclipse Ti2 using a 10× objective quantification, of wound closing was performed by measuring the surface difference between two time points using Nikon software.

Tubulogenesis assay

HUVEC were grown in 200PRF media (ThermoFisher M200PRF500) with Low Serum Growth Supplement (ThermoFisher S00310). Geltrex (ThermoFischer 12760013) was added on $\mu\text{-Slide}$ Angiogenesis (Ibibi 81506), approximately 15 μI per well. Plates were incubated 30 min at 37°C, and 200PRF was added before seeding cells to prevent dehydration. At 70% confluency, cells were detached, seeded, and transduced in wells with media without serum. After an incubation of 24 h, media was replaced by fresh media. Acquisition was performed 24 h later on Nikon Eclipse Ti2 using the 458 nm channel. Quantification was performed with thresholding strategy on ImageJ.

FRET imaging and analysis

Images were acquired with a plan-apochromat 40x water immersion NA 1.1 objective lens on an inverted Zeiss (Oberkochen, Germany) LSM 710 laser scanning microscope. All the images were acquired at 405 nm (donor) and 458 nm (acceptor) excitation wavelengths from an argon laser source, spliced in 32 channels. Intensity images were further processed and analyzed using a custom Python code, which involved background subtraction and removal of saturated pixels, as previously described (Arsenovic et al., 2016). The region of interest was masked manually on Fiji, and the FRET index was calculated by a custom Python code as previously described (Arsenovic et al., 2016, 2017).

Western blotting

Cells were seeded on a six-well plate and lysed on ice with RIPA buffer (Sigma R0278) containing protease and phosphatase inhibitors (ThermoFisher A32959). Standard PAGE and Western blot procedures were employed using the BioRad Trans-Blot 20 Mini-Protean Tetra System, 4%–20% bis-acrylamide cross-linked gels (BioRad 4568096), and polyvinylidene fluoride (PVDF) microporous membranes (GE). Analysis of protein expression was conducted using chemiluminescent images of PVDF membranes captured on the BioRad ChemiDoc Touch Gel Imaging System and associated Image Lab software. Quantification was performed with ImageJ software.

Quantification and statistical analysis

Quantification was done on Fiji software, and statistical significance was calculated using a nonparametric Student's t test integrated in Prism software. All statistical tests were conducted at a 5% significance level (p < 0.05).

ACKNOWLEDGMENTS

We acknowledge funding support from the National Institutes of Health (R35GM119617), the National Science Foundation (CMMI-1653299), and the American Heart Association (16SDG27370007).

REFERENCES

Abiko H, Fujiwara S, Ohashi K, Hiatari R, Mashiko T, Sakamoto N, Sato M, Mizuno K (2015). Rho guanine nucleotide exchange factors involved in cyclic-stretch-induced reorientation of vascular endothelial cells. J Cell Sci 128, 1683–1695.

Alam S, Lovett DB, Dickinson RB, Roux KJ, Lele TP (2014). Nuclear forces and cell mechanosensing. Prog Mol Biol Transl Sci 126, 205–215.

Al-Yafeai Z, Yurdagul A, Peretik JM, Alfaidi M, Murphy PA, Orr AW (2018). Endothelial FN (fibronectin) deposition by $\alpha 5\beta 1$ integrins drives atherogenic inflammation. Arterioscler Thromb Vasc Biol 38, 2601–2614.

Anno T, Sakamoto N, Sato M (2012). Role of nesprin-1 in nuclear deformation in endothelial cells under static and uniaxial stretching conditions. Biochem Biophys Res Commun 424, 94–99.

Armiger TJ, Lampi MC, Reinhart-King CA, Dahl KN (2018). Determining mechanical features of modulated epithelial monolayers using subnuclear particle tracking. J Cell Sci 131, jcs.216010.

Arsenovic PT, Mayer CR, Conway DE (2017). SensorFRET: a standardless approach to measuring pixel-based spectral bleed-through and FRET efficiency using spectral imaging. Sci Rep 7, 15609.

Arsenovic PT, Ramachandran I, Bathula K, Zhu R, Narang JD, Noll NA, Lemmon CA, Gundersen GG, Conway DE (2016). Nesprin-2G, a component of the nuclear LINC complex, is subject to myosin-dependent tension. Biophys J 110, 34–43.

Borghi N, Sorokina M, Shcherbakova OG, Weis WI, Pruitt BL, Nelson WJ, Dunn AR (2012). E-cadherin is under constitutive actomyosin-generated tension that is increased at cell-cell contacts upon externally applied stretch. Proc Natl Acad Sci USA 109, 12568–12573.

Chambliss AB, Khatau SB, Erdenberger N, Robinson DK, Hodzic D, Longmore GD, Wirtz D (2013). The LINC-anchored actin cap connects

- the extracellular milieu to the nucleus for ultrafast mechanotransduction. Sci Rep 3, 1087.
- Chancellor TJ, Lee J, Thodeti CK, Lele T (2010). Actomyosin tension exerted on the nucleus through nesprin-1 connections influences endothelial cell adhesion, migration, and cyclic strain-induced reorientation. Biophys J 99, 115-123.
- Conway DE, Coon BG, Budatha M, Arsenovic PT, Orsenigo F, Wessel F, Zhang J, Zhuang Z, Dejana E, Vestweber D, Schwartz MA (2017). VE-cadherin phosphorylation regulates endothelial fluid shear stress responses through the polarity protein LGN. Curr Biol 27, 2219-2225.
- Conway DE, Breckenridge MT, Hinde E, Gratton E, Chen CS, Schwartz MA (2013). Fluid shear stress on endothelial cells modulates mechanical tension across VE-cadherin and PECAM-1. Curr Biol 23,1024-1030.
- Dahl KN, Ribeiro AJS, Lammerding J (2008). Nuclear shape, mechanics, and mechanotransduction. Circ Res 102, 1307-1318.
- Deguchi S, Maeda K, Ohashi T, Sato M (2005). Flow-induced hardening of endothelial nucleus as an intracellular stress-bearing organelle. J Biomech 38, 1751-1759.
- Grashoff C, Hoffman BD, Brenner MD, Zhou R, Parsons M, Yang MT, McLean MA, Sligar SG, Chen CS, Ha T, Schwartz MA (2010). Measuring mechanical tension across vinculin reveals regulation of focal adhesion dynamics. Nature 466, 263-266.
- Hahn C, Wang C, Orr AW, Coon BG, Schwartz MA (2011). JNK2 promotes endothelial cell alignment under flow. PLoS One 6, e24338.
- Hazel AL, Pedley TJ (2000). Vascular endothelial cells minimize the total force on their nuclei. Biophys J 78, 47-54.
- King SJ, Nowak K, Suryavanshi N, Holt I, Shanahan CM, Ridley AJ (2014). Nesprin-1 and nesprin-2 regulate endothelial cell shape and migration. Cytoskeleton (Hoboken) 71, 423-434.
- Küpper K, Lang N, Möhl C, Kirchgeßner N, Born S, Goldmann WH, Merkel R, Hoffmann B (2010). Tyrosine phosphorylation of vinculin at position 1065 modifies focal adhesion dynamics and cell tractions. Biochem Biophys Res Commun 399, 560-564.
- Lei K, Zhu X, Xu R, Shao C, Xu T, Zhuang Y, Han M (2012). Inner nuclear envelope proteins SUN1 and SUN2 play a prominent role in the DNA damage response. Curr Biol 22, 1609-1615.
- Lombardi ML, Jaalouk DE, Shanahan CM, Burke B, Roux KJ, Lammerding J (2011). The interaction between nesprins and sun proteins at the nuclear envelope is critical for force transmission between the nucleus and cytoskeleton. J Biol Chem 286, 26743-26753.
- Lottersberger F, Karssemeijer RA, Dimitrova N, de Lange T (2015). 53BP1 and the LINC complex promote microtubule-dependent DSB mobility and DNA repair. Cell 163, 880-893.
- Luxton GWG, Gomes ER, Folker ES, Vintinner E, Gundersen GG (2010). Linear arrays of nuclear envelope proteins harness retrograde actin flow for nuclear movement. Science 329, 956-959.
- Mayer CR, Arsenovic PT, Bathula K, Denis KB, Conway DE (2019). Characterization of 3D printed stretching devices for imaging force transmission in live-cells. Cell Mol Bioeng 12, 289-300.

- Morgan JT, Pfeiffer ER, Thirkill TL, Kumar P, Peng G, Fridolfsson HN, Douglas GC, Starr DA, Barakat AI (2011). Nesprin-3 regulates endothelial cell morphology, perinuclear cytoskeletal architecture, and flow-induced polarization. Mol Biol Cell 22, 4324-4334.
- Myat MM, Rashmi RN, Manna D, Xu N, Patel U, Galiano M, Zielinski K, Lam A, Welte MA (2015). Drosophila KASH-domain protein Klarsicht regulates microtubule stability and integrin receptor localization during collective cell migration. Dev Biol 407, 103-114.
- Nguyen BT, Pyun JC, Lee SG, Kang MJ (2019). Identification of new binding proteins of focal adhesion kinase using immunoprecipitation and mass spectrometry. Sci Rep 9, 1-15.
- Petrie RJ, Gavara N, Chadwick RS, Yamada KM (2012). Nonpolarized signaling reveals two distinct modes of 3D cell migration. J Cell Biol 197, 439-455.
- Schürmann S, Wagner S, Herlitze S, Fischer C, Gumbrecht S, Wirth-Hücking A, Prölß G, Lautscham LA, Fabry B, Goldmann WH, et al. (2016). The IsoStretcher: an isotropic cell stretch device to study mechanical biosensor pathways in living cells. Biosens Bioelectron 81, 363-372.
- Shiu JY, Aires L, Lin Z, Vogel V (2018). Nanopillar force measurements reveal actin-cap-mediated YAP mechanotransduction. Nat Cell Biol 20, 262-271.
- Stamatas GN, McIntire LV (2001). Rapid flow-induced responses in endothelial cells. Biotechnol Prog 17, 383-402.
- Stewart RM, Zubek AE, Rosowski KA, Schreiner SM, Horsley V, King MC (2015). Nuclear-cytoskeletal linkages facilitate cross talk between the nucleus and intercellular adhesions. J Cell Biol 209, 403-418
- Tajik A, Zhang Y, Wei F, Sun J, Jia Q, Zhou W, Singh R, Khanna N, Belmont AS, Wang N (2016). Transcription upregulation via force-induced direct stretching of chromatin. Nat Mater 15, 1287-1296.
- Tkachenko E, Gutierrez E, Saikin SK, Fogelstrand P, Kim C, Groisman A, Ginsberg MH (2013). The nucleus of endothelial cell as a sensor of blood flow direction. Biol Open 2, 1007-1012.
- Trepat X, Wasserman MR, Angelini TE, Millet E, Weitz DA, Butler JP, Fredberg JJ (2009). Physical forces during collective cell migration. Nat Phys 5, 426-430.
- Tzima E, Irani-Tehrani M, Kiosses WB, Dejana E, Schultz DA, Engelhardt B, Cao G, DeLisser H, Schwartz MA (2005). A mechanosensory complex that mediates the endothelial cell response to fluid shear stress. Nature 437, 426-431
- Wang N, Tytell JD, Ingber DE (2009). Mechanotransduction at a distance: mechanically coupling the extracellular matrix with the nucleus. Nat Rev Mol Cell Biol 10, 75-82.
- Woychek A, Jones JCR (2019). Nesprin-2G knockout fibroblasts exhibit reduced migration, changes in focal adhesion composition, and reduced ability to generate traction forces. Cytoskeleton 76, 200–208.
- Zhang Q, Narayanan V, Mui KL, O'Bryan CS, Anderson RH, Kc B, Cabe JI, Denis KB, Antoku S, Roux KJ, et al. (2019). Mechanical stabilization of the glandular acinus by Linker of Nucleoskeleton and Cytoskeleton complex. Curr Biol 29, 2826-2839.e4.

Volume 32 August 19, 2021